Spin fluctuations on the verge of a ferromagnetic quantum phase transition in $Ni_3Al_{1-x}Ga_x$

Jinhu Yang,[1,2,*] Bin Chen,[2] Hiroto Ohta,[2] Chishiro Michioka,[2] Kazuyoshi Yoshimura,[2,†]
Hangdong Wang,[1] and Minghu Fang[1,2,‡]
[1]*Department of Physics, Graduate School of Science, Zhejiang University, Hangzhou 310027, China*
[2]*Department of Chemistry, Graduate School of Science, Kyoto University, 606-8502, Japan*
(Received 13 September 2010; revised manuscript received 17 March 2011; published 26 April 2011)

$Ni_3Al_{1-x}Ga_x$ alloys are investigated by the measurements of isothermal magnetization, temperature variations of susceptibilities, and specific heats. Ga doping depresses the ferromagnetic transition temperature (T_C) continuously below the critical point $x = 0.34$. Near the critical region ($x \approx 0.34$), the quantum critical scaling behaviors manifest themselves as the initial susceptibility $\chi^{-1}(T) \propto T^{4/3}$, $T_C^{4/3} \propto (x - x_c)$, and specific heat divided by temperature as $C/T \propto \ln T$ at low temperatures. Furthermore, a novel spin-fluctuation spectrum was discovered in the samples near the quantum critical point, confirming the quantum critical point in this system. The magnetic properties in this system are understood *almost* in terms of the self-consistent renormalization and Takahashi's theory of spin fluctuations.

DOI: 10.1103/PhysRevB.83.134433 PACS number(s): 75.30.Kz, 71.10.Hf, 71.20.Be

I. INTRODUCTION

The quantum phase transition (QPT), which occurs at zero Kelvin, is driven by quantum fluctuations; i.e., zero-point fluctuations, which in contrast to the phase transition occur at finite temperature, are driven by thermal fluctuations. On the threshold of the magnetic ordering, the end point of a second-order phase transition is called quantum critical point (QCP). Although the QPT occurs at absolute zero Kelvin, the quantum spin fluctuation is greatly enhanced and dominates the physical properties of the material near the QCP, resulting in many novel phase diagrams, including non-Fermi liquid behavior[1] and even unconventional superconductivity in some materials.[2,3] The QPTs were first observed experimentally in heavy fermion systems.[1] For example, the paramagnetic metal $CeCu_6$, with a coherent Kondo state at low temperatures, changes into an antiferromagnetic (AF) metal phase in the form of $Ce(Cu_{1-x}Au_x)_6$ for $x > 0.1$ by doping with Au.[4] $YbRh_2Si_2$ is an antiferromagnetic compound with T_N of 70 mK, and its antiferromagnetic ordering is continuously suppressed by the application of a small magnetic field, leading to a field-induced AF QCP.[5]

However, the heavy fermion system often contains strongly correlated $4f$ electrons and some bands of conduction electrons that involve the Kondo interaction and/or the Ruderman-Kittel-Kasuya-Yoshida (RKKY) interaction between the local moments. Compared with the heavy fermion system, $3d$ itinerant magnetic systems have a simpler electronic background without the interplay of itinerant and localized characters. Thus, it is particularly important to study QPT in $3d$ magnetic systems. By using the high-pressure technique, chemical doping, and the external magnetic field, the magnetic transitions were depressed discontinuously toward zero Kelvin in MnSi[6] and $ZrZn_2$[7] and continuously in $NbFe_2$[8] and Ni_3Al.[9] Non-Fermi liquid behaviors were observed in transport properties, such as a $T^{3/2}$ power-law behavior in resistivity in MnSi and $NbFe_2$ and $T^{5/3}$ power-law dependence of resistivity in Ni_3Al.

Ni_3Al is a weak itinerant ferromagnet with the ferromagnetic (FM) transition temperature (T_C) of 41 K at ambient pressure and has a small magnetic ordering moment of 0.075 μ_B/Ni.[10] The resistivity shows $T^{5/3}$ power-law behavior in the vicinity of the T_C, which can be understood within the self-consistent renormalization (SCR) theory of spin fluctuations by taking into account the mode-mode coupling between the different modes of spin fluctuations.[11] In fact, small-angle scattering measurements have been carried out on high-quality specimens of Ni_3Al, discovering that the spin fluctuations are thermally excited near T_C.[12] Furthermore, its T_C decreases with increasing pressure and vanishes in the critical pressure of 8.1 GPa.[9] Theoretical calculations based on the local density approximation (LDA) predicated that the magnetism in the isostructural compound Ni_3Ga is stronger than that in Ni_3Al.[13] It is interesting, however, that Ni_3Ga is a strongly renormalized paramagnet in experimentation.[14] As pointed out by Singh and his coworkers, the magnetic ordering tendency of the compound near the QCP is often overestimated due to neglecting the strong spin fluctuation related to the QCP.[15]

From a structural point of view, it is interesting to study the spin fluctuation by inserting one carbon atom into the body-centered position of the cubic unit cell, which forms Ni_3TC (T = Al and Ga), and the structure changes into an antiperovskite type without changing the space group. Tong *et al.* found that both Ni_3AlC and Ni_3GaC belong to correlated system with enhanced spin fluctuations, which may be due to the instability of the ferromagnetic ordering.[16] Recently, systematic nuclear magnetic resonance (NMR) studies of magnetic properties on Ni_3AlC_x were reported.[17] They found that only 2% carbon substitution destroys the ferromagnetism. Meanwhile, the spin fluctuations of the itinerant electrons dominates the physical properties at low temperatures. In another paper, they studied the intercalation and substitution effect of Si in the Ni_3Al system by means of NMR. The Si intercalation enhances the hyperfine coupling constant and modified the density of states at the Fermi level, as well as the spin fluctuation spectrum near the QCP contrasts to the Si-substituted system.[18]

The ferromagnetic QCPs are generally avoided in favor of the first order transitions in a very clean system or the occurrence of a modulated phase in theory.[19] The chemical-substitution-induced QPT is always accompanied by a disorder that might induce Griffiths phase,[20] which has been, for example, realized in $Ni_{1-x}V_x$ very recently.[21] In this work,

we prepared the polycrystalline samples of $Ni_3Al_{1-x}Ga_x$ (x = 0.0, 0.10, 0.25, 0.30, 0.33, 0.34, 0.40, 0.50, 0.60, and 1.0) by the arc-melting method. We report the first detailed study of the magnetic properties by the measurements of magnetic susceptibilities, isothermal magnetizations, and specific heats. We observe no Griffiths phase in our samples, indicating very little disorder induced by Ga substitution. This is possible due to the substitution of a nonmagnetic atom in our case, in contrast to the $Ni_{1-x}V_x$.[21] The T_C shifts to lower temperatures on increasing the Ga-doping level x and vanishes at a FM QCP of $x_c = 0.34$. The quantum scaling laws are discovered as $T_C^{4/3} \propto (x - x_c)$, and the inverse initial magnetic susceptibility $\chi^{-1}(T) \propto T^{4/3}$. The specific heats divided by temperature are found to follow $C/T \propto \ln T$ in the temperature range of 0.5 to 7 K in samples with x = 0.33 and 0.34, giving further evidence for the occurrence of quantum criticality in this system. Furthermore, η, the inverse coefficient of the fourth term of the Landau free energy expansion, displaying a peak-like behavior at low temperatures and low magnetic fields in the samples near QCP, strongly supports the quantum criticality in this system. The spin fluctuations in this system can be described *almost* by the self-consistent renormalization theory and Takahashi's theory of spin fluctuations.

II. EXPERIMENTAL

Polycrystalline samples of $Ni_3Al_{1-x}Ga_x$ (x = 0.0, 0.10, 0.25, 0.30, 0.33, 0.34, 0.40, 0.50, 0.60, and 1.0) were synthesized by an Ar arc-melting method. The original materials were Ni ball (3N), Al ingot (4N), and Ga ball (5N). Each sample was melted repeatedly by inverting six times to improve the homogeneity. The as-cast buttons were annealed at 1050°C for ten days in evacuated quartz tubes. The weight loss was found below 1% during above processes. It is very difficult to synthesize the sample with $T_C \leqslant 10$ K. We made over 15 samples in the range of $0.30 \leqslant x \leqslant 0.40$ and just succeeded in obtaining three samples with T_C less than 10 K. This is probably due to the fact that the magnetic properties of the Ni_3Al system are highly sensitive to the Ni content, since only 3% deficiency of Ni atom can drive Ni_3Al system from a ferromagnet with a T_C of 41 K to an nonmagnetic compound.[10] Therefore, even a negligible amount of Ni or Al weight loss still has great impact on the magnetic properties in substituted samples, especially on the threshold of the magnetic ordering.

The DC magnetic properties of the samples were measured by using a Quantum Design Magnetic Physical Properties Measurement System (PPMS). The magnetic susceptibilities were measured under 1 kOe in the process of zero-field cooling (ZFC). In some cases, the maximum magnetic field we applied is 3, 4, 6, or 8 T for isothermal magnetization measurements. The specific heat measurements were performed on a Quantum Design PPMS-14.

III. RESULTS

A. Temperature dependence of magnetic susceptibility in $Ni_3Al_{1-x}Ga_x$

Figure 1 shows the temperature dependence of magnetic susceptibilities ($\chi = M/H$) of the polycrystalline $Ni_3Al_{1-x}Ga_x$ (x = 0, 0.10, 0.25, 0.30, 0.33, 0.34, 0.40, 0.50, 0.60, and 1.0) below 100 K under an applied magnetic field of 1 kOe. In the parent sample Ni_3Al, the ferromagnetic phase transition is characterized by a sudden increase in χ below $\approx$ 50 K and then tends to saturate at low temperatures. This is a typical process of the ferromagnetic phase transition. With increasing Ga-doping level x, the T_C is suppressed to lower temperatures and becomes obscure for $x > 0.40$. The suppression of T_C has been realized by applying an external pressure in this system.[9] Since the radius of the Ga atom is larger than that of Al, it is natural to expect higher T_C in samples with larger lattice constant. However, another important effect, as reported by Singh and his coworkers, is the quantum spin fluctuations in this system.[15] The quantum spin fluctuation was thought to be enhanced gradually from Ni_3Al toward Ni_3Ga. In that case, the quantum spin fluctuation would be enhanced greatly on Ga doping, especially near QCP, and thus can completely destroy the long-range magnetic ordering in this system. In the temperature range of 100–300 K, the χ data can be well fitted to the modified Curie-Weiss law as

$$\chi(T) = \chi_0 + \frac{C}{T-\theta} = \chi_0 + \frac{N_0 P_{\text{eff}}^2}{3k_B(T-\theta)}, \qquad (1)$$

where χ_0 denotes the temperature-independent term, C the Curie constant, N_0 the number of magnetic atoms, k_B the Boltzmann constant, P_{eff} the effective moment of Ni atom,

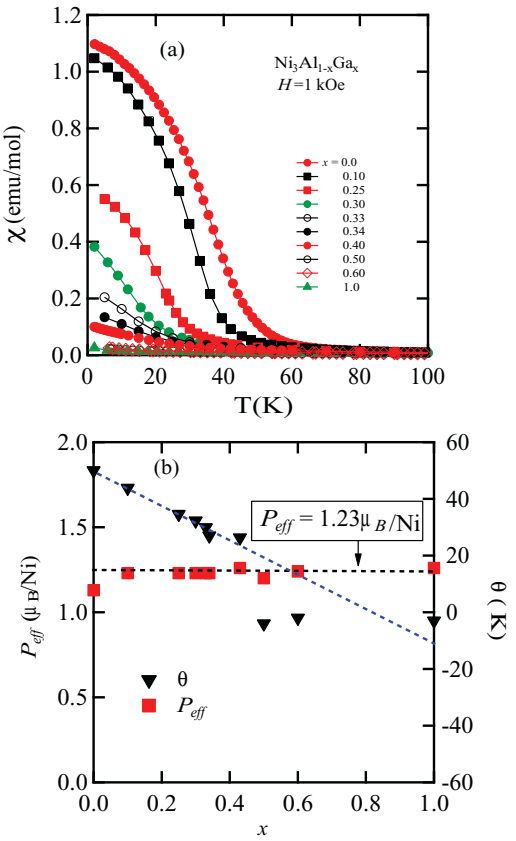

FIG. 1. (Color online) (a) Temperature dependence of ZFC magnetic susceptibilities $\chi(= M/H)$ for $Ni_3Al_{1-x}Ga_x$ samples (x = 0.0, 0.10, 0.25, 0.30, 0.33, 0.34, 0.40, 0.50, 0.60, and 1.0) under the DC magnetic field of 1 kOe. (b) The effective magnetic moment P_{eff} and the Weiss temperature θ as a function of x. The dashed lines are guides to the eyes.

and θ the paramagnetic Curie temperature, i.e., the Weiss temperature. The refined parameters are $C = 0.48$ emu K/mol and $\theta = 50$ K for the parent compound Ni_3Al. The estimated effective moment (P_{eff}) is almost independent of sample $\approx 1.23\mu_B$ per Ni atom, while the θ decreases with increasing Ga content x and becomes a negative value for samples $x \geqslant 0.50$ as displayed in Fig. 1(b).

B. Isothermal magnetization, Arrott plots, and magnetic phase diagram of $Ni_3Al_{1-x}Ga_x$

Figures 2 and 3 show the results of our magnetic measurements for $Ni_3Al_{1-x}Ga_x$ in forms of isothermal magnetization

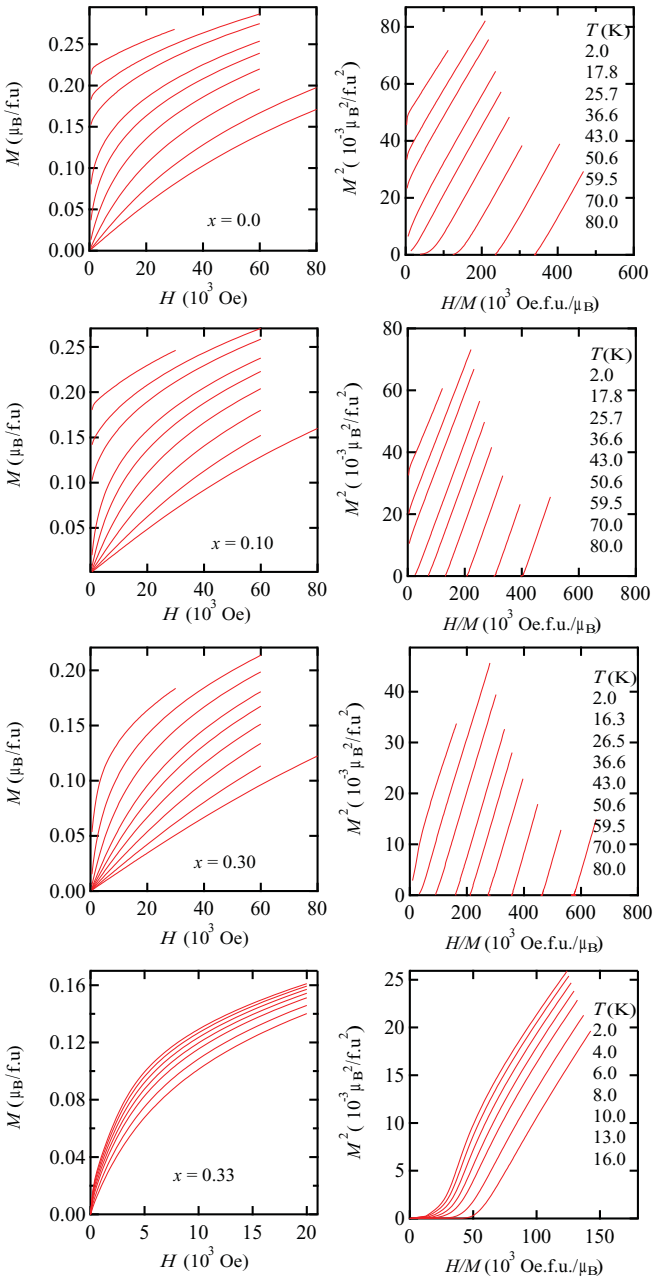

FIG. 2. (Color online) (Left) The isothermal magnetization of $Ni_3Al_{1-x}Ga_x$ alloys ($x = 0.0$, 0.10, 0.30, 0.33) at different temperatures and the corresponding Arrott plot, i.e., M^2 vs. H/M plots are on the right side of the panel.

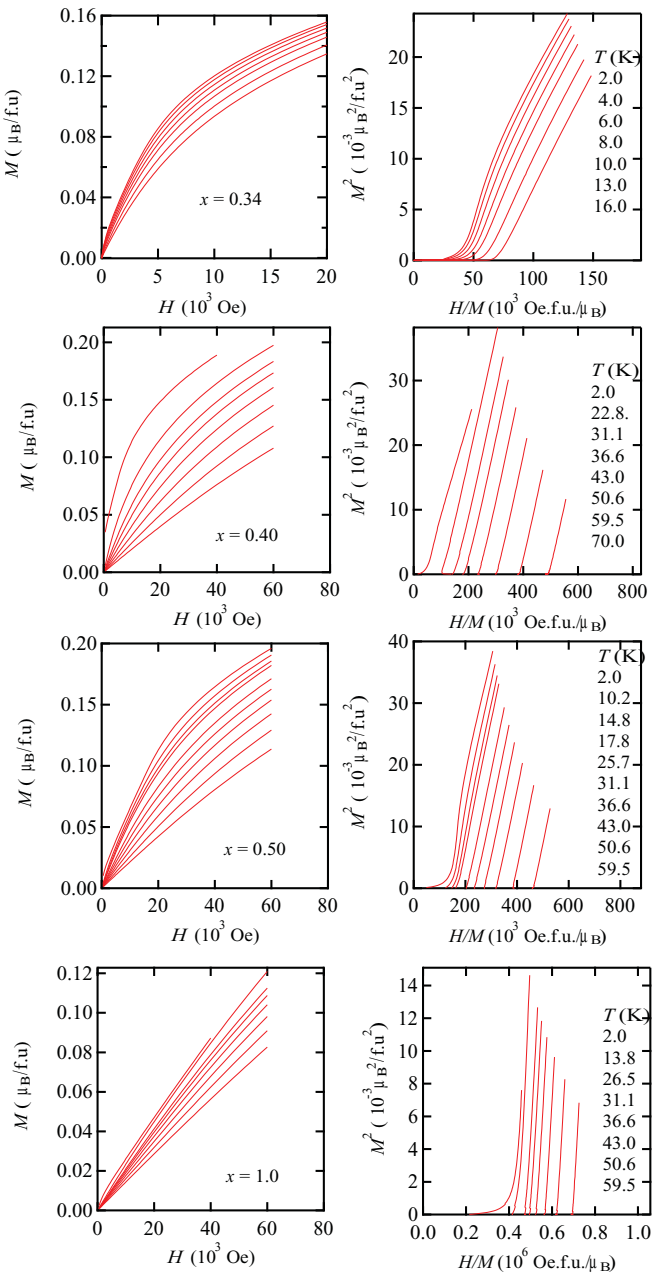

FIG. 3. (Color online) (Left) The isothermal magnetization of $Ni_3Al_{1-x}Ga_x$ alloys ($x = 0.34$, 0.40, 0.50, and 1.0) at different temperatures and the corresponding Arrott plots (right).

$M(H)$ curves and Arrott plots at different temperatures (the data are not shown all for clarity). The Arrott plots of $Ni_3Al_{1-x}Ga_x$ are in good forms of $M(H,T)^2 = M(0,T)^2 + \eta H/M(H,T)$, exhibiting a wide range of linear behavior in the high magnetic-field side. This behavior is a characteristic of itinerant electron-weak ferromagnets. Similar behavior has been discovered in other weak itinerant ferromagnetic systems, for example, $Y(Co_{1-x}Al_x)_2$,[22] $Sr_{1-x}Ca_xRuO_3$,[23] and $ZrZn_2$.[24] It is convenient to obtain T_C precisely for a weak ferromagnetic system by using the Arrott plots method, since the extrapolated line from the high magnetic-field region goes through the origins at just T_C. In fact, the extrapolated line for each sample

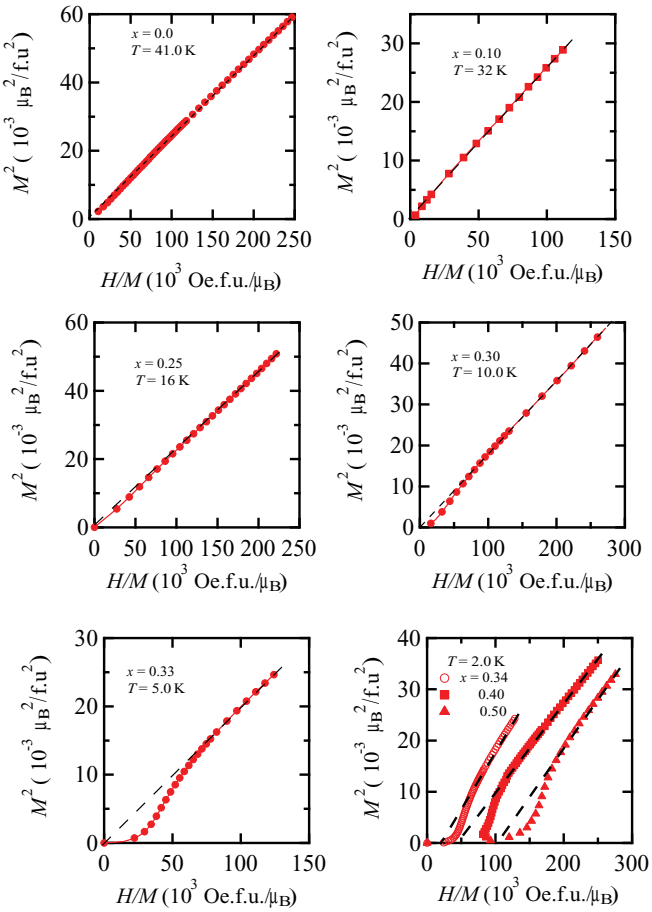

FIG. 4. (Color online) Arrott plots for ferromagnetic samples with $x = 0.0$, 0.10, 0.25, 0.30, and 0.33 at the temperature of their T_Cs. and for paramagnetic samples with $x = 0.34$, 0.40, and 0.50 at the temperature of 2 K. The dashed lines are fit linearly in the high magnetic fields for each sample.

at T_C from the linear part of the Arrott plots all go through the origins as shown in Fig. 4. The samples with $x \geqslant 0.34$ are in paramagnetic states above 2 K, which is our low-temperature limit (the data are not shown all for clarity). It is clear that T_C was continuously depressed on Ga doping from 41 K ($x = 0.0$) to 5 K ($x = 0.30$) and vanishes near x_c =0.34, which is expected to be a quantum critical point as shown in Fig. 5. The ferromagnetic phase line obeys the scaling law as $T_C^{(d+n)/z} \propto (x - x_c)$,[6,25,26] where, in our case, $d = 3, z = n + 2 = 3$ for a 3D ferromagnetic system. Due to the limited number of data points, it is not possible to obtain the exponent in the scaling law by fitting. However, $T_C^{4/3}$ shows good linear behavior dependence of the Ga-doping level x as shown in the upside of Fig. 5. Similar scaling laws were also discovered in other weak itinerant ferromagnetic systems near the critical point; for example, the Nb-substituted system of $Zr_{1-x}Nb_xZn_2$,[27] or MnSi under high pressure for $P \leqslant P^* = 12$ kbar.[6]

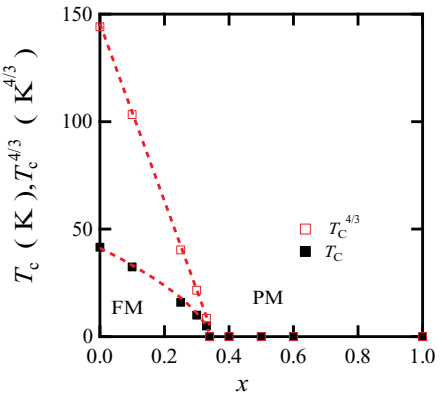

FIG. 5. (Color online) Magnetic phase diagram of $Ni_3Al_{1-x}Ga_x$ alloys. FM: ferromagnetic state; PM: paramagnetic state. The dashed lines are to guide the eyes.

The Rhodes-Wohlfarth ratio, defined as P_c/P_s, where $P_c(P_c + 2) = P_{\text{eff}}^2$ and P_s spontaneous moment, is expected larger than the unity for an itinerant ferromagnetic system. As the results, the ratios of P_{eff}/P_s and P_c/P_s increase with increasing Ga levels and are well exceeding the unity,

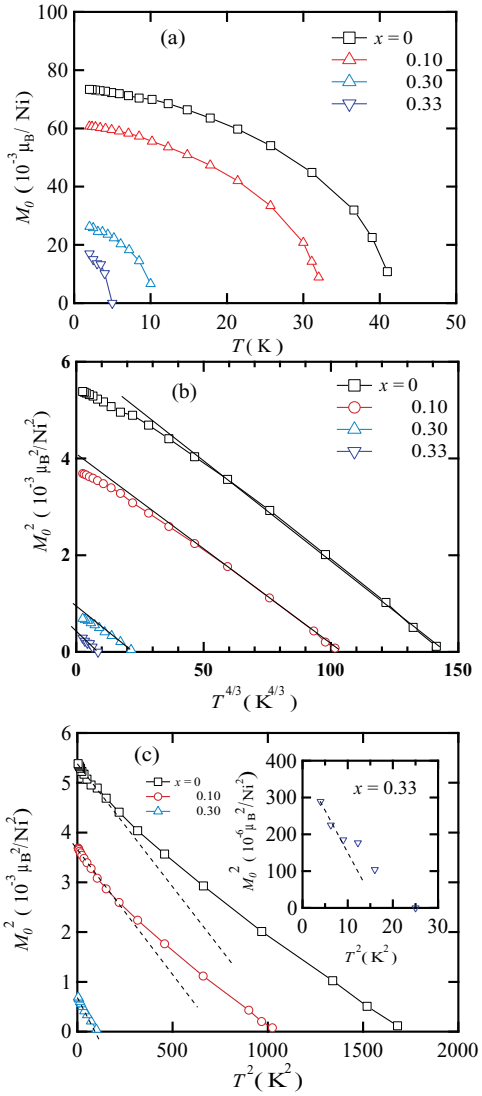

FIG. 6. (Color online) Temperature dependence of spontaneous magnetization for samples with $x = 0.0$, 0.10, and 0.30. (a) $M_0(T)$ against T, (b) $M_0^2(T)$ against $T^{4/3}$, and (c) $M_0^2(T)$ against T^2, Inset: $M_0^2(T)$ against T^2 for sample with $x = 0.33$. The solid (dashed) lines are to guide the eyes.

TABLE I. Magnetic parameters of $Ni_3Al_{1-x}Ga_x$. T_C, P_s, and $P_{\rm eff}$ are ferromagnetic phase transition temperature, spontaneous magnetization at ground state, and effective moment, respectively.

Sample	T_C (K)	P_s (μ_B/Ni)	$P_{\rm eff}$ (μ_B/Ni)	P_c (μ_B/Ni)	$P_{\rm eff}/P_s$	P_c/P_s
0	41	0.075	1.13	0.45	15.1	6.0
0.10	33	0.063	1.23	0.48	19.5	7.6
0.30	10	0.028	1.23	0.48	43.9	17.1
0.33	5	0.020	1.23	0.48	61.5	24.0

indicating a typical itinerant electron-weak ferromagnetism in this system. The parameters estimated are summarized in Table I.

At temperatures around T_C in samples with $x = 0.0$ and 0.10, the $M(H)$ curves are convex, which are due to the critical-spin fluctuation excited by thermal fluctuations as suggested by the small-angle neutron scattering measurements in Ni_3Al.[12] With decreasing temperature, such spin fluctuations are weakened as the $M(H)$ shows almost linear dependence on magnetic field at 2 K, indicating that thermal spin fluctuations are dominant in the case of $x \leqslant 0.10$. However, the convex shape of $M(H)$ curves not only appears near T_C but also survives at 2 K in samples with $x = 0.30$ and 0.33, suggesting

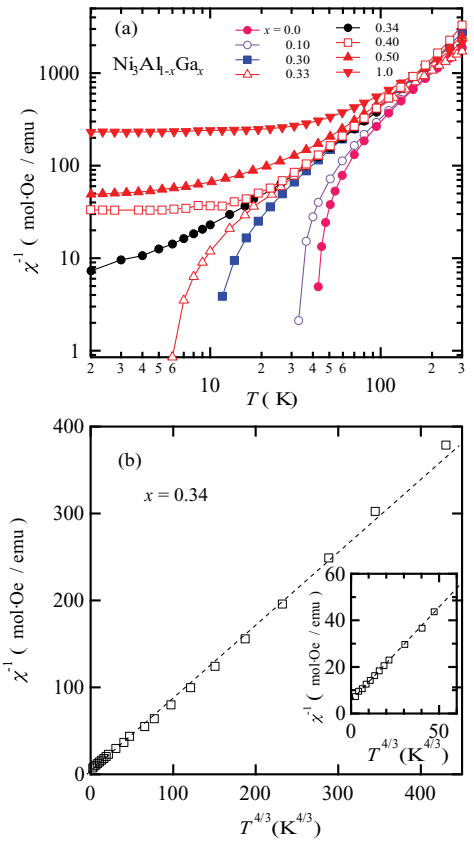

FIG. 7. (Color online) Temperature dependence of the initial magnetic susceptibility for $Ni_3Al_{1-x}Ga_x$ samples ($x = 0$, 0.10, 0.30, 0.33, 0.34, 0.40, 0.50, and 1.0): (a) $\chi^{-1}(T)$ as a function of temperature T in a double logarithm; (b) $\chi^{-1}(T)$ as a function of $T^{4/3}$ for sample with $x = 0.34$. An enlarged view of the low temperature region is shown in the inset. The dashed line is to guide the eyes.

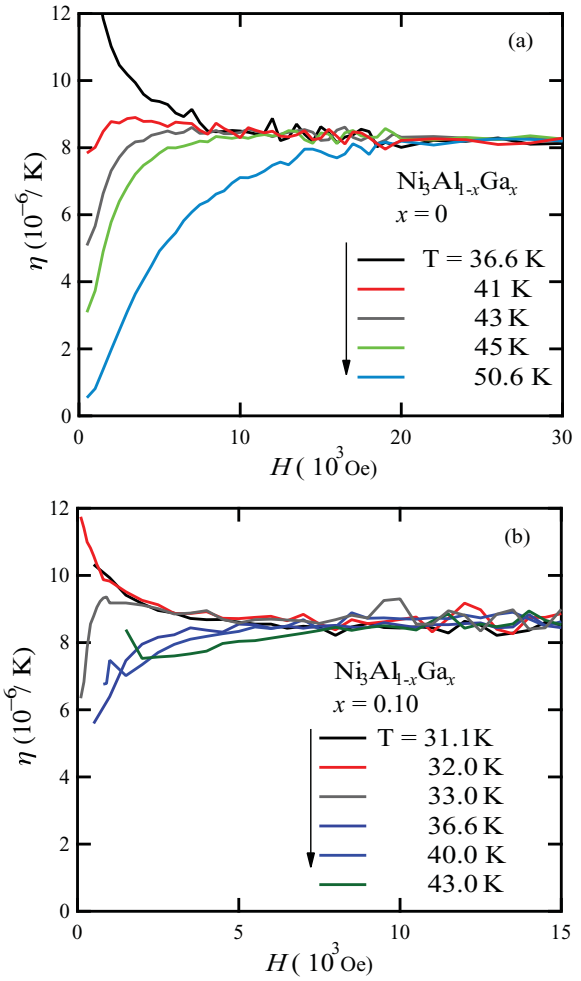

FIG. 8. (Color online) η as a function of the external magnetic field H at variety temperatures for (a) $x = 0.0$ and (b) $x = 0.10$.

this kind of spin fluctuation is not excited by thermal fluctuations, at least totally. The convexities of $M(H)$ at low temperatures are also discovered in the paramagnetic samples with $x = 0.34$ and 0.40 and tend to disappear in samples with further increasing Ga level. This scenario strongly supports that such kind of spin fluctuation is related to the QCP in this system.

On the other hand, the spontaneous magnetization $M_0(T) = \lim_{H\to 0} M(H,T)$ and the initial susceptibility $\chi(T) = \lim_{H\to 0} M(H,T)/H$ were determined by extrapolating the data from the linear part of the Arrott plots. The results of the spontaneous magnetization as a function of temperature with different exponents are given in Fig. 6. The spontaneous magnetizations in the ground state $M_0(0)$ were estimated as $0.075\mu_B(x = 0.0)$, $0.063\mu_B(x = 0.10)$, $0.028\mu_B(x = 0.30)$, and $0.020\mu_B(x = 0.33)$ per Ni atom by extrapolating the data $M_0(T)$ to zero temperature, indicating that Ga doping suppresses $M_0(0)$. In the temperature near T_C, M_0^2 shows $T^{4/3}$ behavior near T_C in Fig. 6(b) as predicted by the SCR theory of spin fluctuations and converts to T^2 law at low temperatures in Takahashi's spin fluctuation theory if the spin-wave contribution is small enough.[11,29] The temperature dependence of the initial susceptibility χ(T) is displayed in

Fig. 7. The χ diverges at T_C in the ferromagnetic samples ($x \leqslant 0.33$). For the samples with $x \geqslant 0.34$, χ(T) approaches a constant as the temperature tends toward zero. Near the QCP, the samples with $x = 0.34$ exhibit a good scaling law as $\chi^{-1} \propto T^{4/3}$ behavior up to 100 K as shown in Fig. 7(b), as expected near a QCP.[25] This means the sample with $x = 0.34$ is the nearest one to the QCP among the samples prepared in this system.

In the framework of a weakly ferromagnetic limit, the coupling between different modes of the spin-fluctuation spectrum has an essential effect on the physical properties of the system. Murata and Doniach suggested that the fourth-order term of the Landau expansion of the free energy in terms of uniform magnetization contains the mode-mode coupling term.[28] Generally, the mode-mode coupling in the model referred to by the authors is temperature dependent due to thermal excitation of spin fluctuations, but the effective coupling constant is independent of T and q vector. The mode-mode coupling is invariable as described in terms of the coefficient of the fourth-order term $\bar{F}_{10}$. Apparently, it is true that $\eta(H)$ ($\bar{F}_{10} = 1/\eta$), which were estimated as $dM^2/d(H/M)$ for samples with $x = 0.0$ and 0.10 in high magnetic fields, are independent of temperature as shown in Fig. 8. It is worth noting that from the low-field side, η decreases (increases) quickly to a constant value if the temperature below (above) the T_C with increasing magnetic field. Furthermore, at T_C, η is independent of the magnetic field, indicating this kind of mode-mode coupling is mainly excited by thermal spin fluctuations, which is in agreement with the analysis of isothermal magnetization results above.

However, the mode-mode coupling strength displays peak-like behavior for samples near the QCP in low magnetic fields and at low temperatures. We emphasize our main results in Fig. 9. For example, a peak appears in the η at low $T = 2.0$ K, although the sample for $x = 0.30$ shows ferromagnetic ordering below 10 K contrasts to other samples with ferromagnetic ordering [see Fig. 8(a)]. In high magnetic field, η is nearly independent of magnetic field and becomes a constant, similar to the results for $x = 0.0$ and 0.10. According to Takahashi's theory, $\eta = 15T_0/4k_BT_A^2$, where k_B is Boltzmann constant, and T_0 and T_A are the *spectral widths* of the dynamical spin fluctuation spectrum and the dispersion of the dynamical magnetic susceptibility in wave-vector and energy space, respectively.[29] The peaks due to the enhancement of T_0 and decrease of T_A, with increasing magnetic fields at low temperatures and low magnetic fields (the field is less

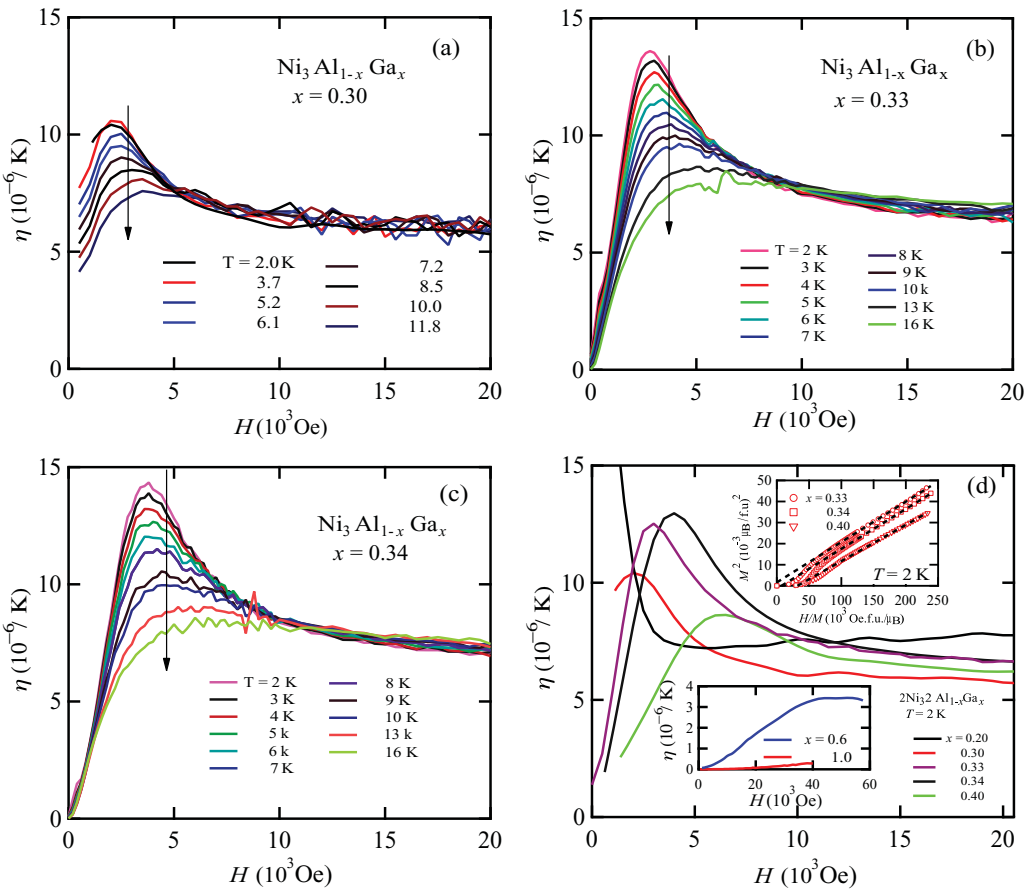

FIG. 9. (Color online) η as a function of the external magnetic field H at different temperatures for (a) $x = 0.30$, (b) $x = 0.33$, (c) $x = 0.34$. (d) η as a function of the external magnetic field H at 2 K for samples with $x = 0.10$, 0.30, 0.33, 0.34, and 0.40. In the cases with $x = 0.60$ and 1.0, ηs are shown in the lower inset. The upper inset shows the Arrott plot for the samples with $x = 0.33$, 0.34, and 0.40 very near QCP in the low-temperature limit of 2 K. The dashed lines are fit linearly in the high magnetic fields, indicating that the sample $x = 0.34$ is the nearest one on the verge of the QCP in this system.

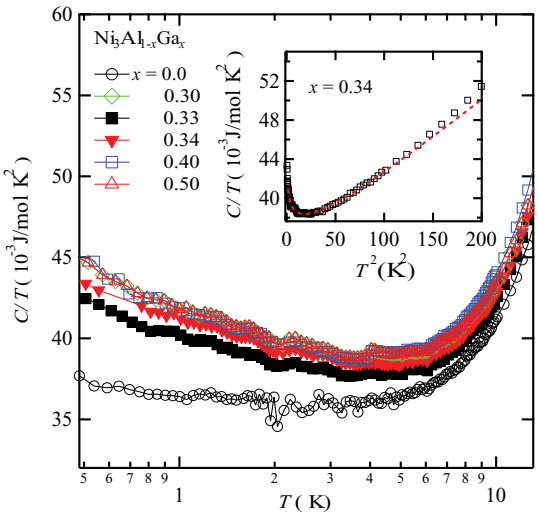

FIG. 10. (Color online) C/T as the function of the logarithm of the temperature for samples with $x = 0.0$, 0.30 0.33, 0.34, 0.40, and 0.50. A typical fit to the SCR theory in the sample with $x = 0.34$ in the dashed line are shown in the inset.

than 2 kOe, as for the $x = 0.33$ case), indicate that the main part of the excited spin fluctuations are located in a narrower energy space and in a wider wave-vector space. The magnetic field works as probing the magnitude of the energy of the spin fluctuations. Herein, we suggest that the driving force of such spin fluctuations is not of thermodynamic, at least totally, but quantum critical-like, since this peak vanishes quickly when the system departures from the QCP [see Fig. 9(d)].

Measurements of the specific heats give further evidence for the existence of QCP in this system. We present the results of the specific heat experiments in samples with $x = 0.0$, 0.30, 0.33, 0.34, 0.40, and 0.50 in Fig. 10. For pure sample with $x = 0.0$, C/T shows very weak enhancement with decreasing temperature. However, for samples with $x = 0.30$, 0.33, 0.34, 0.4, and 0.50), $C/T \propto \ln T$ at low temperatures as expected for a FM QCP.[30] These results suggest the ferromagnetic spin fluctuations are enhanced for the samples close to the QCP in this system.

IV. DISCUSSION

In order to understand the spin fluctuations in this system, we will discuss our experimental results on the basis of SCR theory, which takes the spin-fluctuation effect into account in a self-consistent way, as follows. Recently, Takahashi expanded SCR theory by assuming a conservation of the summation of the zero-point spin fluctuations and thermal spin fluctuations.[29] In Takahashi's theory, T^2 dependence of the spontaneous moment at low temperatures obeys the formula[31]

$$\left[\frac{M_0(0,T)}{M_0(0)}\right]^2 = 1 - \frac{50.4}{M_0(0)^4}\left(\frac{T}{T_A}\right)^2. \tag{2}$$

The spin fluctuation at low temperatures is described in terms of T_A by neglecting the spin-wave contribution. Furthermore, $\bar{F}_{10}$ can also be obtained from η in Arrott plots. Takahashi gave the relations

$$\left(\frac{T_c}{T_0}\right)^{5/6} = \frac{\sqrt{30C_z}M_0(0)^2}{40C_{4/3}}\left(\frac{\bar{F}_{10}}{T_C}\right)^{1/2}, \tag{3}$$

$$\left(\frac{T_c}{T_A}\right)^{5/3} = \frac{M_0(0)^2}{20C_{4/3}}\left(\frac{2}{15C_z}\right)^{1/3}\left(\frac{T_c}{\bar{F}_{10}}\right)^{1/3}. \tag{4}$$

We choose the values of the integral constants $C_{4/3}$ and C_z as 1.006 and 0.50, respectively, for the estimation of T_A and T_0. The estimated parameters are listed in Table II. T_A estimates from Eq. (2) are 3.6(0.1), 4.2(0.1), 8.3(0.3), and 7.8(0.3) $\times 10^4$ (K) for the sample with x = 0, 0.10, 0.30, and 0.33, respectively, which are self-consistent and comparable to the values estimated by other means on SCR theory. The parameters estimated for x = 0 are similar to the previous report.[18] In SCR theory, the inverse magnetic susceptibility is expressed as the equation

$$y = 1 + \eta^* K_0^2 \int_0^{1/K_0} dz z^3 \left[\ln u - \frac{1}{2u} - \psi(u)\right], \tag{5}$$

where $y = \chi(0)/\chi$, $u = z(z^2 + y)/t$, $K_0^2 = 1/2\alpha T_A \chi(0)$, $\eta^* = 15\bar{F}_{10}T_0/2(\alpha T_A)^2$, and $(1-\alpha)^{-1}$ is the Stoner enhancement factor. The α is often estimated $\approx$1 for ferromagnetic or nearly ferromagnetic materials. $t = T/T^*$, $T^* = T_0 K_0^3$, and $\psi(u)$ is the digamma function. The parameter value of $\bar{F}_{10}$ was derived experimentally from η, the inverse slope of the Arrott plots at high magnetic fields.

TABLE II. Spin-fluctuation parameters of $Ni_3Al_{1-x}Ga_x$. T_C and $\bar{F}_{10}$ are derived from the Arrott plots. T_0 and T_A are calculated according to SCR theory. In samples with $x = 0.34$ and 0.40, marked with an asterisk, data are derived from the fits to the specific heat data on SCR theory and the corresponding value of T_A are derived from the relationship $\bar{F}_{10} = 4k_B T_A^2/15T_0$. The T_0^*, T_A^*, and $\bar{F}_{10}^*$ are the best fits to the initial magnetic susceptibility data on SCR theory.

Sample	T_C	T_0	T_A	$\bar{F}_{10}$	T_0^*	T_A^*	$\bar{F}_{10}^*$
(x)	(K)	(10^3 K)	(10^4 K)	(10^5 K)	(10^3 K)	(10^4 K)	(10^5 K)
0	41	2.7	3.7	1.36(0.01)	3.3(0.1)	5.9(0.1)	2.82(0.01)
0.10	32	2.9	3.7	1.26(0.02)	1.8(0.1)	4.3(0.1)	2.71(0.01)
0.30	10	2.6	4.0	1.63(0.02)	2.6(0.2)	5.5(0.1)	3.14(0.02)
0.33	5	2.5	3.5	1.34(0.01)	2.8(0.2)	4.9(0.2)	2.33(0.02)
0.34	—	1.3*	2.6	1.42(0.01)	1.8(0.1)	3.0(0.1)	1.26(0.01)
0.40	—	1.2*	2.7	1.63(0.01)	1.2(0.1)	3.1(0.1)	2.07(0.03)

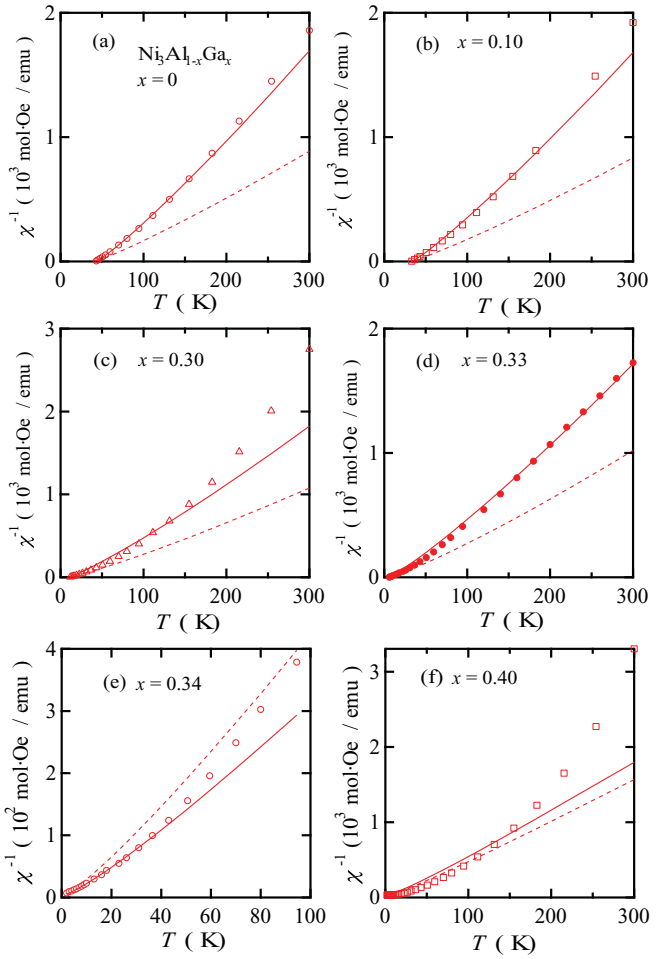

FIG. 11. (Color online) Temperature dependence of the inverse magnetic susceptibilities χ^{-1} of the samples with $x = 0.0, 0.10, 0.30, 0.33, 0.34$, and 0.40. The dashed lines stand for the calculated inverse magnetic susceptibilities based on the SCR theory, and the solid lines are the best fits to each experimental data by the theory.

Therefore, the calculated temperature dependence of the inverse magnetic susceptibilities for $x \leqslant 0.33$ by Eq. (5), using the parameters T_0, T_A, $\bar{F}_{10}$, and $M_0(0)$ obtained from the experiment, are shown by dashed lines in Fig. 11. The dashed lines show clear deviations at high temperatures but agree well with the experimental data at low temperatures. If we allow the parameters T_0, T_A, and $\bar{F}_{10}$ to be changeable, we can obtain the best fits to each sample as shown by the solid lines in Fig. 11. As a result, the parameters of T_0^*, T_A^*, and $\bar{F}_{10}^*$ are a little larger than the values obtained from the Arrott plots, however, in the same order of magnitude. For the paramagnetic samples with $x = 0.34$ and 0.40, the T_0 are derived from the fits to the specific heat on the SCR theory.[32] The parameters of T_0 and T_A, derived from Arrott plots and the initial magnetic susceptibility and specific heat on the SCR and Takahashi's theory, can be found to be in the same order, indicating that the spin fluctuations of this system can be understood *almost* within the frameworks of both the SCR theory and Takahashi's theory of spin fluctuations.

V. CONCLUSION

In summary, we provide convincing experimental evidence for the occurrence of FM QCP in $Ni_3Al_{1-x}Ga_x$ at the critical concentration of $x_c = 0.34$. The quantum critical behavior manifests itself by the scaling law as $T_C^{4/3} \propto (x - x_c)$, the initial susceptibility $\chi^{-1}(T) \propto T^{4/3}$ and the specific heat divided by temperature $C/T \propto \ln T$ near the QCP. The spontaneous magnetic moment $M_0(T)^2$ obeys $T^{4/3}$ behavior near T_C and converts to T^2 law at low temperatures. Furthermore, the novel quantum spin fluctuations spectrum at low magnetic fields and low temperatures were discovered in samples near the QCP ($x = 0.30, 0.33, 0.34$, and 0.40), which also strongly supports the presence of quantum criticality in this system. Overall, the spin fluctuation in this system can be understood *almost* in the frameworks of SCR theory and Takahashi's theory of ferromagnetic spin fluctuations.

ACKNOWLEDGMENTS

This research was supported by the National Science Foundation of China (Grant Nos. 10974175, 10874146, 10934005), and the National Basic Research Program of China (Grant No. 2009CB929104), the PCSIRT of the Ministry of Education of China (Grant No. IRT0754). The work in Kyoto University was supported by a Grant-in-Aid for the Global COE Program of Kyoto University "International Center for Integrated Research and Advanced Education in Materials Science" and Scientific Research on Priority Area "Invention of anomalous quantum materials" (No. 16076210) from the Ministry of Education, Culture, Sports, Science and Technology of Japan, and also by Grants-in-Aid for Scientific Research (Nos. 19350030 and 22350029) from the Japan Society for Promotion of Science.

*yangjinhu@kuchem.kyoto-u.ac.jp
†kyhv@kuchem.kyoto-u.ac.jp
‡mhfang@zju.edu.cn

[1] G. R. Stewart, Rev. Mod. Phys. **73**, 797 (2001), and references therein.
[2] N. D. Mathur, F. M. Grosche, S. R. Julian, I. R. Walker, D. M. Freye, R. K. W. Haselwimmer, and G. G. Lonzarich, Nature (London) **394**, 39 (1998).
[3] S. S. Saxena, P. Agarwal, K. Ahilan, F. M. Grosche, R. K. W. Haselwimmer, M. J. Steiner, E. Pugh, I. R. Walker, S. R. Julian, P. Monthoux, G. G. Lonzarich, A. Huxley, I. Sheikin, D. Braithwaite, and J. Flouquet, Nature (London) **406**, 587 (2000).
[4] H. v. Lohneysen, T. Pietrus, G. Portisch, H. G. Schlager, A. Schroder, M. Sieck, and T. Trappmann, Phys. Rev. Lett. **72**, 3262 (1994).

[5]J. Custers, P. Gegenwart, H. Wilhelm, K, Neumaier, Y. Tokiwa, O. Trovarelli, C. Geibel, F. Steglich, C. Pepin, and P. Coleman, Nature (London) **424**, 524 (2003).

[6]C. Pfleiderer, G. J. McMullan, S. R. Julian, and G. G. Lonzarich, Phys. Rev. B **55**, 8330 (1997). MnSi is a ferromagnet with helical moment, and the QCP is avoided as the magnetic phase transition turns into 1st order in the pressure range $P^* < P < P_C$ where $P^* =$ 12 kbar and the critical pressure $P_C = 14.6$ kbar. However, it still can be argued why, away from the masked QCP, MnSi shows weakly ferromagnetic behavior.

[7]M. Uhlarz, C. Pfleiderer, and S. M. Hayden, Phys. Rev. Lett. **93**, 256404 (2004).

[8]M. Brando, W. J. Duncan, D. Moroni-Klementowicz, C. Albrecht, D. Gruner, R. Ballou, and F. M. Grosche, Phys. Rev. Lett. **101**, 026401 (2008).

[9]P. G. Niklowitz, F. Beckers, G. G. Lonzarich, G. Knebel, B. Salce, J. Thomasson, N. Bernhoeft, D. Braithwaite, and J. Flouquet Phys. Rev. B **72**, 024424 (2005). It should be point out that, in this article, the authors observed a T^2 regime in resistivity well below 1 K and very close to the critical pressure, which indicated the phase transition becomes a very weak one.

[10]F. R. Boer, C. J. Schinkel, J. Biesterbros, and S. Proost, J. Appl. Phys. **40**, 1049 (1969).

[11]T. Moriya, *Spin Fluctuations in Itinerant Electron Magnetism* (Springer, Berlin, 1985), and references therein.

[12]N. R. Bernhoeft, G. G. Lonzarich, P. W. Mitchell, and D. McK. Paul, Phys. Rev. B **28**, 422 (1983).

[13]A. Aguayo, I. I. Mazin, and D. J. Singh, Phys. Rev. Lett. **92**, 147201 (2004).

[14]S. M. Hayden, G. G. Lonzarich, and H. L. Skriver, Phys. Rev. B **33**, 4977 (1986).

[15]I. I. Mazin and D. J. Singh, Phys. Rev. B **69**, 020402(R) (2004); A. Aguayo and D. J. Singh, *ibid.* **66**, 020401(R) (2002).

[16]P. Tong, Y. P. Sun, X. B. Zhu, and W. H. Song, Phys. Rev. B **74**, 224416 (2006); **73**, 245106 (2006).

[17]B. Chen, C. Michioka, Y. Itoh, and K. Yoshimura, J. Phys. Soc. Jpn. **77**, 103708 (2008).

[18]B. Chen, H. Ohta, C. Michioka, and K. Yoshimura, J. Phys. Soc. Jpn. **79**, 064707 (2010).

[19]D. Belitz and T. R. Kirkpatrick, Phys. Rev. Lett. **89**, 247202 (2002), and references therein.

[20]T. Vojta and J. Schmalian, Phys. Rev. B **72**, 045438 (2005); T. Vojta, C. Kotabage, and J. A. Hoyos, *ibid.* **79**, 024401 (2009).

[21]S. Ubaid- Kassis, T. Vojta, and A. Schroeder, Phys. Rev. Lett. **104**, 066402 (2010).

[22]K. Yoshimura and Y. Nakamura, Solid State Commun. **56**, 767 (1985); K. Yoshimura, M. Takigawa, Y. Takahashi, H. Yasuoka, and Y. Nakamura, J. Phys. Soc. Jpn. **56**, 1138 (1987); K. Yoshimura, M. Mekata, M. Takigawa, Y. Takahashi, and H. Yasuoka, Phys. Rev. B **37**, 3593 (1988).

[23]Y. Itoh, T. Mizoguchi, and K. Yoshimura, J. Phys. Soc. Jpn. **77**, 123702 (2008); T. Kiyama, K. Yoshimura, K. Kosuge, H. Mitamura, and T. Goto, *ibid.* **68**, 3372 (1999); K. Yoshimura, T. Imai, T. Kiyama, K. R. Thurber, A. W. Hunt, and K. Kosuge, Phys. Rev. Lett. **83**, 4397 (1999).

[24]E. A. Yelland, S. J. C. Yates, O. Taylor, A. Griffiths, S. M. Hayden, and A. Carrington, Phys. Rev. B **72**, 184436 (2005).

[25]A. J. Millis, Phys. Rev. B **48**, 7183 (1993).

[26]S. R. Julian, J. Phys. Condens. Matter **8**, 9675 (1996).

[27]D. A. Sokolov, M. C. Aronson, W. Gannon, and Z. Fisk, Phys. Rev. Lett. **96**, 116404 (2006).

[28]K. K. Murata and S. Doniach, Phys. Rev. Lett. **28**, 295 (1972).

[29]Y. Takahashi, J. Phys. Soc. Jpn. **55**, 3553 (1986); J. Phys. Condens. Matter **4**, 3611 (1992); Y. Takahashi and T. Sakai, *ibid.* **7**, 6279 (1995).

[30]U. Zulicke and A. J. Millis, Phys. Rev. B **51**, 8996 (1995).

[31]T. Kanomata, T. Igarashi, H. Nishihara, K. Koyama, K. Watanabe, K.-U. Neumann, and K. R. A. Ziebeck, Mater. Trans. **47**, 496 (2006), and reference therein.

[32]R. Konno and T. Moriya, J. Phys. Soc. Jpn. **56**, 3270 (1987).